# Avoiding hologram bending in photorefractive crystals

**A. A. Freschi, P. M. Garcia, I. Rasnik, and J. Frejlich**

*Laboratório de Óptica, Instituto de Física, Universidade Estadual de Campinas, 13083-970 Campinas-SP, Brazil*

**K. Buse**

*Fachbereich Physik, Universität Osnabrück, Barbarastrasse 7, D-49069 Osnabrück, Germany*

Received June 14, 1995

Dynamic coupled-wave theory predicts the bending of recorded hologram phase planes in most photorefractive crystals. Bent holograms occur in $LiNbO_3$ and other photovoltaic crystals that are particularly interesting as holographic storage media and result in a reduced overall diffraction efficiency. We show that hologram bending in $LiNbO_3$ can be avoided or at least sensibly reduced by use of an actively stabilized recording technique. © 1996 Optical Society of America

Holographic recording in photorefractive materials in general produces amplitude and phase coupling of the incident interfering beams.[1] The bending of the hologram phase planes arises from phase coupling, and this effect is present in photorefractive holograms having a phase shift $\phi$ between the light pattern and the refractive-index grating that is different from $\pm\pi/2$. In photovoltaic crystals such as $LiNbO_3$, where nearly $\pi$-shifted holograms are produced,[2] the phase plane displacement is a linear function of the crystal depth so that a tilted hologram as a special case of bent holograms results. Hologram bending was recently directly measured in $LiNbO_3$.[3] The bending of the phase planes produces an out-of-Bragg hologram, and the efficiency for diffraction of the recording beams is accordingly reduced. Such diffraction efficiency reduction represents a considerable handicap in the use of photovoltaic materials such as $LiNbO_3$ as holographic memories. In this Letter we show that hologram bending in photovoltaic materials can be avoided or at least strongly reduced by the use of an actively stabilized recording technique.

We carried out the holographic recording using a new technique[4] that is schematically represented in Fig. 1. One of the recording beams is phase modulated with phase amplitude $\psi_d$ and angular frequency $\Omega$ using a piezoelectric-supported mirror. The intensity measured behind the crystal along the $I_S$ direction shows a dc and several harmonic terms in $\Omega$. The dc term is $I_S^{\mathrm{dc}} = [I_S^0(1-\eta) + I_R^0\eta + 2J_0(\psi_d)\sqrt{I_S^0 I_R^0}\sqrt{\eta(1-\eta)}\cos\varphi]T$, whereas the amplitude of the first harmonic is $I^{\Omega} = 4J_2(\psi_d)T\sqrt{I_S^0 I_R^0}\sqrt{\eta(1-\eta)}\sin\varphi$ and that of the second harmonic is $I^{2\Omega} = 4J_2(\psi_d)T\sqrt{I_S^0 I_R^0}\sqrt{\eta(1-\eta)}\cos\varphi$. Similar expressions are found for the $I_R$ direction. Here $I_S^0$ and $I_R^0$ are the intensities of both incident beams, $T$ is the overall transmittance including bulk absorption and Fresnel reflection effects, $\eta$ is the diffraction efficiency of the hologram, $\varphi$ is the phase between the transmitted and the diffracted beams behind the crystal, and $J_0$, $J_1$, and $J_2$ are Bessel functions of orders 0, 1, and 2, respectively. The terms $I^{\Omega}$ and $I^{2\Omega}$ detected at $D_S$ are separated with suitable bandpass filters. The $\Omega$-frequency signal is frequency doubled and phase shifted, whereas the original $2\Omega$-frequency signal is amplified, so that a couple of 90°-shifted signals $V_1 = V_0\sin(\varphi)\sin(2\Omega t + \varepsilon)$ and $V_2 = V_0\cos(\varphi)\cos(2\Omega t + \varepsilon)$ can be obtained, with $V_0 = 4J_1(\varphi_d)k_E T\sqrt{I_S^0 I_R^0}\sqrt{\eta(1-\eta)}$, where $k_E$ is the photodetector and signal-processing electronics response constant and $\varepsilon$ is a phase delay arising from the optoelectronic circuitry. The signals $V_1$ and $V_2$ are then added to form the expression $V_+ = V_0\cos(2\Omega t - \varphi + \varepsilon)$. A two-phase lock-in amplifier tuned to $2\Omega$ is used for measuring the amplitudes of the $X$ component, $V_X = V_0\sin(\varphi - \varepsilon - \theta)$, and the $Y$ component, $V_Y = V_0\sin(\varphi - \varepsilon - \theta)$, of the $2\Omega$-frequency signal $V_+$, referred to an arbitrarily $\theta$-shifted lock-in reference signal. The reference system's phase $\theta$ can be chosen to cancel the remaining

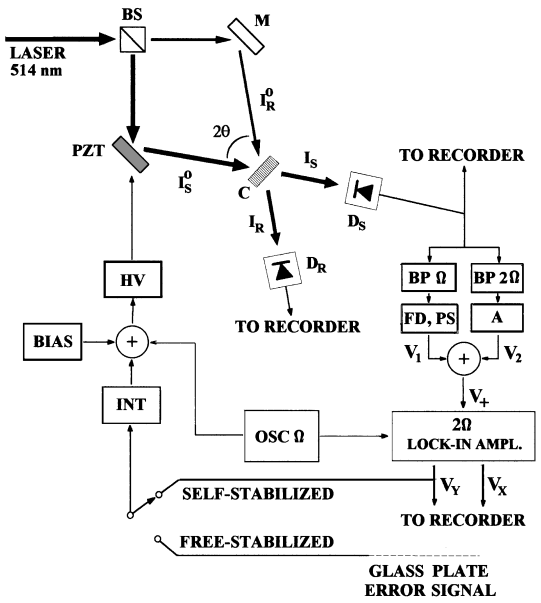


Fig. 1. Actively stabilized holographic recording and measurements setup. BS, beam splitter; M, mirror; PZT, piezoelectric-supported mirror; C, Fe-doped $LiNbO_3$ crystal; $D_S$, $D_R$, photodetectors; BP's, bandpass filters; FD, frequency doubler; PS, phase shifter; A, amplifier; OSC Ω, oscillator at frequency Ω; INT, integrator; HV, high-voltage source.

0146-9592/96/020152-03$6.00/0 

phase delay term $\varepsilon$ ($\varepsilon + \theta = 0$), where the value of $\varepsilon$ to be offset can be computed from the lock-in measurement of $V_1$ or $V_2$, so $V_X$ and $V_Y$ can be written as

$$V_X = \pm V_0 \sin \varphi , \qquad V_Y = \pm V_0 \cos \varphi . \tag{1}$$

From the signals above and the expressions for the dc terms in $I_S$ and $I_R$ the following relations are obtained:

$$V_X^2 + V_Y^2 = \left[16 J_1^2(\psi_d) k_E^2 T^2 I_S^0 I_R^0\right] \eta (1 - \eta) , \tag{2}$$

$$\tan \varphi = \pm V_X / V_Y , \tag{3}$$

$$I_S^{\mathrm{dc}} - I_R^{\mathrm{dc}} = \left[\left(I_S^0 - I_R^0\right)(1 - 2\eta) + 4 J_0(\psi_d) \times \sqrt{I_S^0 I_S^0}\sqrt{\eta(1 - \eta)} \cos \varphi \right] T . \tag{4}$$

The simultaneous solution of Eqs. (2)–(4) unequivocally determines the evolution of $\eta$ and $\varphi$.

For nonbent holograms $\varphi$ is related in a simple way ($\varphi = \phi \pm \pi/2$) to the holographic phase shift $\phi$.[5] Thus for a nonbent $\pi/2$-shifted hologram $\varphi = 0$ (or $\pi$), yielding $V_X = 0$, so that this term can be used as an error signal for stabilization purposes. In this case the holographic setup is actively fixed to $\varphi = 0$ or $\varphi = \pi$, depending on the way that the electronics in the loop is set. Each time a phase perturbation in the setup shifts $\varphi$ away from the preset value 0 (or $\pi$) the signal $V_X$ shifts away from zero and a corresponding correction voltage is applied to the piezoelectric mirror via its high-voltage amplifier, so that the optical path length in the setup is modified until the stable equilibrium condition $\varphi = 0$ (or $\pi$) is restored.[6] For materials exhibiting holographic bending instead, the relation between $\varphi$ and $\phi$ is not a simple one, as $\varphi$ evolves during recording and neither $V_X$ nor $V_Y$ can be used as an error signal for stabilized recording of the nonperturbated hologram. However, if recording is carried out on a photovoltaic $LiNbO_3$ crystal (exhibiting $\phi \approx \pi$) with interfering beams of equal intensity, phase coupling can be reduced so that a nonbent hologram is produced.[7] In this case $\varphi = \pm\pi/2$ and $V_Y = 0$ so that $V_Y$ is a suitable error signal for stabilization purposes. In general experimental conditions, however, bending does occur in photovoltaic crystals so that $V_Y \neq 0$.

Experiments are carried out with a $d = 0.85$ mm thick 0.1-wt% Fe-doped $LiNbO_3$ crystal. Figure 1 shows the setup used. The sample is illuminated by two extraordinarily polarized laser beams symmetrically entering the crystal with an incident angle of $\theta = 15.8°$ in air. One beam is phase modulated with amplitude $\psi_d = 0.5$ rad and an angular frequency $\Omega = 2\pi \times 2.0$ kHz. The wave vector **K** of the interference pattern is aligned parallel to the **c** axis of the crystal, and the surfaces perpendicular to the **K** vector are short-circuited. The frequency bandwidth of the stabilization system is approximately 10 Hz. Two different kinds of experiment were carried out. In one case the holographic setup was actively stabilized using the reflected and transmitted beams from a small plate of glass placed just by the side of the crystal with an additional detector and lock-in amplifier not shown in Fig. 1. This is called a free-stabilized recording because the holographic setup is stabilized but the recording on the crystal is not perturbated or forced in any way. In the second case the holographic setup was stabilized on the crystal itself by the interference of the transmitted and diffracted beams behind the crystal.[4] This is called a self-stabilized recording because the hologram being recorded is at the same time the reference for stabilization.

The evolution of $V_X$ and $V_Y$ measured in free-stabilized experiments were recorded and are displayed in Fig. 2(a) for $\beta^2 = I_R^0/I_S^0 \ll 1$. Also shown are the evolution of the dc terms $I_S^{\mathrm{dc}}$ and $I_R^{\mathrm{dc}}$ (to show the extent of energy exchange) and their sum $I_S^{\mathrm{dc}} + I_R^{\mathrm{dc}}$ (to evaluate the amount of light scattering). The experimental data are corrected for light scattering and substituted into Eqs. (2)–(4) to permit the evolution of $\eta$ and $\varphi$ to be computed. The solid curves in Fig. 3(a) show $\eta$ and $\varphi$ as calculated from the data in Fig. 2(a). The dashed curves in Fig. 3(a) show the results for an experiment with $\beta^2 \gg 1$. In both cases the diffraction efficiency never increases above ≈70% (as high as ≈50% for $\beta^2 \ll 1$ and ≈67% for $\beta^2 \ll 1$). Note the evolution of $\varphi$ during recording, as a consequence of hologram bending. The evolution occurs in opposite directions for $\beta^2 \gg 1$ and for $\beta^2 \ll 1$, showing that in these conditions bending occurs in opposite directions, too.

Experiments in similar conditions were repeated in the self-stabilized regime: The holographic setup was stabilized with the hologram in the crystal itself used as a reference. The output voltage $V_Y$ is used as the error signal for the stabilization loop so that it is forced to be zero (so that $\varphi$ is kept fixed to $\pi/2$, which is the value corresponding to a $\pi$-shifted and nonbent hologram) throughout the whole recording process. The evolutions of $V_X$, $V_Y$, $I_S^{\mathrm{dc}}$, and $I_S^{\mathrm{dc}} + I_R^{\mathrm{dc}}$ are shown in Fig. 2(b) for $\beta^2 \ll 1$. The solid curve in Fig. 3(b) shows $\eta$ calculated from data in Fig. 2(b), whereas the

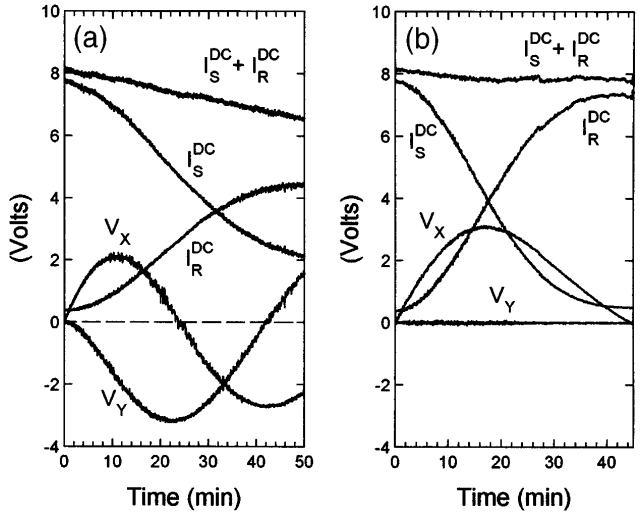


Fig. 2. Evolution of $V_X$, $V_Y$, $I_S^{\mathrm{dc}}$, $I_R^{\mathrm{dc}}$, and $I_S^{\mathrm{dc}} + I_R^{\mathrm{dc}}$ for (a) free-stabilized recording with $\beta^2 = 1/21$ and $I_R^0 + I_S^0 \approx$ 3.7 mW/cm$^2$ and (b) self-stabilized recording with $\beta^2 = 1/21$ and $I_S^0 + I_R^0 \approx 3.7$ mW/cm$^2$.

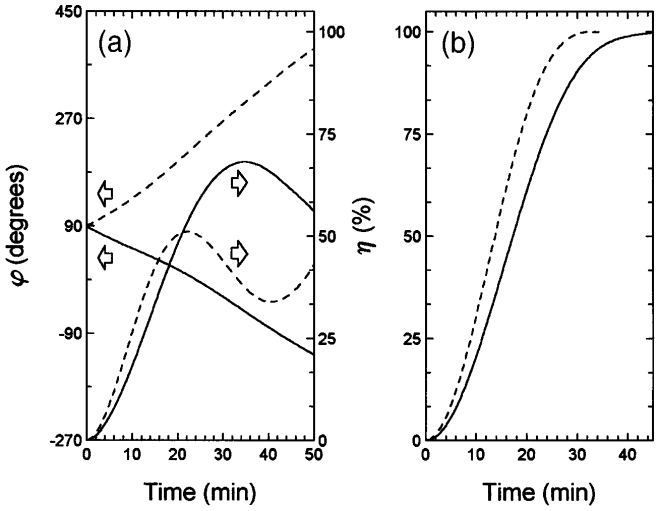


Fig. 3. (a) Evolution of $\eta$ and $\varphi$ during free-stabilized recording for $\beta^2 = 1/21$ (solid curves) with $I_R^0 + I_S^0 \approx 3.7$ mW/cm$^2$ and for $\beta^2 = 15$ (dashed curves) with $I_R^0 + I_S^0 \approx 4.0$ mW/cm$^2$. (b) Evolution of $\eta$ during self-stabilized recording for $\beta^2 = 1/21$ (solid curve) with $I_R^0 + I_S^0 \approx 3.7$ mW/cm$^2$ and for $\beta^2 = 17$ (dashed curve) with $I_R^0 + I_S^0 \approx 4.0$ mW/cm$^2$.

dashed curve shows the result for a similar experiment with $\beta^2 \gg 1$.

In the experiments reported here for photovoltaic $LiNbO_3$, $\eta$ is computed from $I_S^{dc}$, $I_R^{dc}$, $V_X$, and $V_Y$, which are measured behind the crystal. The overall transmittance term $T$ accounts for bulk absorption and Fresnel reflection effects, so these effects are excluded in the calculated value for $\eta$. Holographic recording in the free-stabilized mode always yields diffraction efficiencies much lower than 100% because the hologram becomes off Bragg with respect to the recording beams. In the self-stabilized mode, however, stationary 100% diffraction efficiencies[7] are achieved in spite of the large ratios between the input intensities. This indicates that a sensible reduction in hologram bending has actually been obtained.

The 100% diffraction efficiencies are achieved when the phase $\varphi$ between the transmitted and the diffracted beams behind the crystal is forced to be fixed at the value ($\varphi = \pm\pi/2$) that it should have for the case of a nonbent $\pi$-shifted photovoltaic hologram. In these conditions we observe a continuous movement (with a speed of approximately 0.02 grating period/min) of the interference pattern onto the crystal. This fact indicates that a nonstationary mechanism is involved. For our experimental conditions ($K \approx 6.7 \times 10^6$ m$^{-1}$) and the known parameters for the crystal,[8] the steady-state intensity amplification is estimated to be approximately $\exp(\Gamma d) \approx 1.8$, where $\Gamma \propto E_D$ is the exponential gain coefficient[8] and $E_D$ is the diffusion field. The amplification factor is approximately 1 order of magnitude lower than the experimental values computed from the maximum ratio for $I_i^{dc}(t)/I_i^{dc}(0)$ (with $t$ the time and $i = S, R$) ranging from approximately 6 to 20 for the four free- and self-stabilized experiments reported here with $\beta^2 \gg 1$ and $\beta^2 \ll 1$. Such a large difference shows that energy exchange in these materials is not controlled by the diffusion field $E_D$ but is probably produced because of a transient phase shift slightly deviating from the steady-state $\phi = \pi$ value. The direction of this deviation is apparently always controlled by the relative position of the high- and low-intensity beams, and that is the reason why the weak beam is always amplified regardless of the orientation of the **c** axis.[9] The comparatively large transient energy exchange occurring in these conditions can be qualitatively explained by a small transient variation in the hologram phase shift throughout the crystal thickness. This causes an imaginary part of the space-charge field originating from the photovoltaic effect. Because in Fe-doped $LiNbO_3$ the photovoltaic field is much larger than the diffusion field, its influence can predominate over diffusion. In this way even a small phase deviation from $\phi = \pi$, which can occur even in the self-stabilized regime, may produce a large energy exchange.

We have shown that it is possible to avoid or at least sensibly reduce hologram bending in photovoltaic $LiNbO_3$ crystals by the use of self-stabilized recording techniques. In these conditions 100% diffraction efficiency is always achieved, even if the recording is carried out with beams of widely different light intensities. Because of bending effects, considerably lower diffraction efficiency values are achieved if holograms are recorded without any constraints.

This research was partially supported by the Conselho Nacional de Desenvolvimento Científico e Tecnológico, the Coordenadoria de Aperfeiçoamento de Pessoal de Ensino Superior, the Financiadora de Estudos e Projetos, and Volkswagen-Stiftung (Germany).

## References

1. N. V. Kukhtarev, V. B. Markov, S. G. Odulov, M. S. Soskin, and V. L. Vinetskii, Ferroelectrics **22,** 949 (1979).
2. R. Rupp, Appl. Phys. B **41,** 153 (1986).
3. S. Tao, Z. H. Song, and D. R. Selviah, Opt. Commun. **108,** 144 (1994).
4. A. A. Freschi and J. Frejlich, Opt. Lett. **20,** 635 (1995).
5. D. L. Staebler and J. J. Amodei, J. Appl. Phys. **43,** 1042 (1972).
6. P. A. M. dos Santos, L. Cescato, and J. Frejlich, Opt. Lett. **13,** 1014 (1988).
7. A. A. Freschi and J. Frejlich, J. Opt. Soc. Am. B **11,** 1837 (1994).
8. P. Günter and J.-P. Huignard, eds., *Photorefractive Materials and Their Applications I and II,* Vols. 61 and 62 of Topics in Applied Physics (Springer-Verlag, Berlin, 1988).
9. N. V. Kukhtarev, V. B. Markov, and S. G. Odulov, Opt. Commun. **23,** 338 (1977).